RESEARCH ARTICLE

Macromolecular Materials and Engineering
Open Access
www.mame-journal.de

Biomedical Efficacy of Garlic-Extract-Loaded Core-Sheath Plasters for Natural Antimicrobial Wound Care

*Hamta Majd, Merve Gultekinoglu, Cem Bayram, Beren Karaosmanoğlu, Ekim Z. Taşkıran, Didem Kart, Özgür Doğuş Erol, Anthony Harker, and Mohan Edirisinghe**

This work explores the application of *Allium sativum* (Garlic) extract, in the creation of novel polymeric core-sheath fibers for wound therapy applications. The core-sheath pressurized gyration (CS PG) technology is utilized to mass-produce fibers with a polycaprolactone (PCL) core and a polyethylene oxide (PEO) sheath, loaded with garlic extract. The produced fibers maintain structural integrity, long-term stability and provide a cell-friendly surface with rapid antibacterial activity. The physical properties, morphology, therapeutic delivery, cytotoxicity, thermal and chemical stability of PCL, PEO, PEO/Garlic, Core-Sheath (CS) PEO/PCL and PEO/Garlic/PCL fibers are analyzed. Findings show that the addition of garlic extract greatly increases the fibers' thermal durability, while decreasing their diameter, thus improving cell adhesion and proliferation. In-vitro release tests reveal a rapid release of garlic extract, which has significant antibacterial action against both Gram-negative *Escherichia coli* (*E. coli*) and Gram-positive *Staphylococcus aureus* (*S. aureus*) bacteria species. Cell viability experiments validate the fiber samples' biocompatibility and nontoxicity, making them appropriate for integrative medicine applications. These core-sheath structures emphasize the potential of combining natural therapeutic agents with advanced material technologies to develop cost-effective, sustainable and highly effective wound dressings, offering a promising solution to the growing concerns associated with conventional synthetic antibacterial agents.

1. Introduction

Wound healing is a complex process requiring materials and methods that are biocompatible and capable of withstanding the threat posed by developing bacteria resistance,[1] particularly in the context of minor wounds that are treated outside of healthcare settings. Despite advances in the disciplines of pharmacology and material sciences, the search for the perfect wound-healing treatment continues; it is driven by the need for solutions that use natural resources but with minimal environmental effects. Naturopathic medicine uses natural substances to provide therapeutic properties such as antibacterial, antioxidant and anti-inflammatory actions, which are essential for enhancing the wound healing process.[2–4] Despite their effectiveness, synthetic antimicrobial agents, have shown substantial limitations that impact both patient care and global health, necessitating a need for safer, more sustainable options. The rapid growth of antibiotic resistance resulted in the rise of multidrug resistance bacteria, which carries the potential to

H. Majd, M. Edirisinghe
Department of Mechanical Engineering
University College London
London WC1E 7JE, UK
E-mail: m.edirisinghe@ucl.ac.uk

M. Gultekinoglu, C. Bayram
Department of Nanotechnology & Nanomedicine Division
Institute for Graduate Studies in Science & Engineering Hacettepe University
Ankara 06800, Turkey

B. Karaosmanoğlu, E. Z. Taşkıran
Department of Medical Genetics
Faculty of Medicine
Hacettepe University
Ankara 06230, Turkey

D. Kart
Department of Pharmaceutical Microbiology
Faculty of Pharmacy
Hacettepe University
Ankara 06230, Turkey

Ö. D. Erol
Department of Medical Biology
Faculty of Medicine
Hacettepe University
Ankara 06230, Turkey

A. Harker
Department of Physics
Astronomy
University College London
London WC1E 6BT, UK

The ORCID identification number(s) for the author(s) of this article can be found under https://doi.org/10.1002/mame.202400014

DOI: 10.1002/mame.202400014

pose significant challenges to public health. Additionally, the cytotoxic properties of synthetic agents, especially those derived from heavy metals such as silver and copper, could damage cells and slow the healing process, limiting their use in wound care.[5,6] Not only this, but environmental concerns are also rising; the manufacture, use and disposal of synthetic antimicrobials contribute to ecological damage. In comparison to synthetic therapeutic products, natural therapeutics offer new approaches to treat skin disorders, addressing challenges such as high production costs, extended manufacturing delays and rising bacterial resistance.[7]

Allium sativum, more commonly known as garlic, has been valued globally for thousands of years for its health and therapeutic benefits.[8] Being rich in sulfur compounds, enzymes, amino acids and minerals such as selenium, garlic yields the highest concentration of sulfur compounds within its Allium species.[9] The distinctive scent of garlic, as well as its numerous therapeutic properties, can be attributed to these compounds. Allicin (diallyl thiosulfinate or diallyl disulfide), one of the most active substances in garlic, is produced when the garlic bulb is crushed or chopped. This activates the enzyme alliinase that metabolizes alliin to allicin which is further broken down into vinyldithiines.[10,11] However, this is not the case for all forms of garlic; in comparison to powdered or freshly crushed garlic, processed forms such as garlic oil, aged garlic and steamed-distilled garlic lack significant levels of alliin or allicin.[12] Studies have shown that garlic has numerous benefits for physical health, owing to its anti-inflammatory, anti-clotting and immune-boosting properties.[13,14] Due to its antibiotic activity (thiosulfinates), it has a strong antibacterial effect against both *Gram-positive* and *Gram-negative* bacteria, as well as the ability to decrease platelet aggregation.[15,16]

Driven by its allicin component garlic's antibacterial activity works differently than other antibacterial agents such as graphene, silver, copper and gold nanoparticles.[17,18] Silver nanoparticles physically eliminate bacteria by adhering to and penetrating the cell wall, which generates an excess of free radicals and reactive oxygen species that inhibit cell development;[19] similarly, copper nanoparticles generate reactive oxygen species in bacteria, peroxidizing lipids, oxidizing proteins and damaging DNA;[20] gold nanoparticles damage the cell's membrane potential, leading to a reduction in cellular metabolism.[21] In contrast, allicin suppresses thiol-containing enzymes like cysteine proteinases, alcohol dehydrogenases and thioredoxin reductases essential for maintaining and balancing the metabolism in microorganisms.[22] The inflammatory phase, which involves the body's first response to injury, is a vital stage in the wound healing process, if prolonged, it can delay healing and increase the chance of infection. Recent studies have shown that garlic extract can help terminate the inflammatory stage of healing rapidly, while also increasing fibroblast and fibrocyte proliferation, promoting collagen deposition, thereby enhancing wound healing.[23]

The combination of natural healing agents and advanced material technologies has resulted in the development of novel wound care treatments. Among them, core-sheath (CS) polymeric fibers, owing to their high surface area and versatility in functionalization, provide an effective scaffold for drug administration and wound healing.[24] These fibers are made up of a core material encased within a sheath material, offering a multifunctional structure for advanced wound care solutions.[25] Moreover, the flexibility of using two polymers with different solubilities (hydrophilic-hydrophobic) or sources (natural-synthetic) enables the delivery of therapeutic agents at various times, therefore making it ideal for treating wounds during different healing stages through multidrug release systems.

Owing to its superior mechanical properties and biodegradable characteristics, polycaprolactone (PCL) is an ideal material for applications in tissue engineering and drug delivery.[26] However, it lacks biological recognition sites and generates insufficient micromovement for cell attachment, thereby restricting its usability.[27–29] Polyethylene oxide (PEO), a nontoxic, biocompatible polymer, inhibits protein adhesion and has been used as an anti-inflammatory polymeric coating for numerous implanted biomaterials.[30,31] A coating of PEO on PCL in a core-sheath fiber structure can improve the aqueous characteristics and biocompatibility of PCL, thereby modulating the interaction between cells and materials.[32,33] Additionally, encapsulating a natural antimicrobial agent into the PEO sheath can enhance the fibers' functionality by stimulating antimicrobial surface activity.

The area of advanced wound care represents a major challenge in terms of fiber fabrication techniques specifically for the effective delivery of therapeutic agents. It is essential that methods are not only precise but industrially relevant and sustainable. The core-sheath pressurized gyration (CS PG) is a novel fiber production process which overcomes the drawbacks of other conventional fiber production techniques, distinguished by its ability to extrude core and sheath materials through concentric orifices in a pressurized gyration system. This method provides precise control over fiber morphology and the distribution of the active ingredients within the fibers.[34,35] It addresses the scalability limitations of traditional manufacturing techniques such as coaxial electrospinning.

This study aims to utilize the natural therapeutic properties of garlic in a novel polymeric core-sheath fiber structure using a scalable manufacturing technique, to improve the healing of minor wounds in a natural and cost-effective manner. The core-sheath structure consists of a PCL core for mechanical strength and long-term stability, with a PEO sheath to maintain a cell-friendly surface, while ensuring the rapid release of active molecules to prevent microbial growth. By combining modern engineering with naturopathic medicine, the fibers produced in this study have the potential to be used as plasters for minor cuts and wounds. In this research, the potential of core-sheath polymeric fibers for multifunctional wound dressings has been investigated, focusing on morphology, physical form, antibacterial activity, cell viability and in-vitro release behavior.

2. Experimental Section

2.1. Materials

Polyethylene oxide (PEO) powder (M_W 2×10^5 g mol^{-1}) and polycaprolactone (PCL) pellets (M_W 8×10^4 g mol^{-1}) were obtained from Sigma Aldrich (UK). Ground garlic powder (Allium sativum 100% pure) used for antibacterial agent extraction was purchased from Just Ingredients (UK). Chloroform was used as a solvent for producing both polymer solutions. Additionally, it was used in a

binary system with acetone as the primary solvent for the garlic extraction process. Phosphate buffer saline (PBS, pH = 7.4) was used as a buffer solution, along with deionized water, for in-vitro studies, which was acquired from Oxoid ThermoFischer (UK).

2.2. Polymer Solution Preparation

The polymer solution for the core of the fibers involved dissolving PCL pellets into virgin chloroform to make a concentration of 15% w/v. The polymer solution prepared for the sheath of the fibers involved mixing PEO powder with garlic extract, which contained chloroform/acetone (80:20) to make a concentration of 15% w/v. All solutions were magnetically stirred for 24 h at ambient temperature of (≈23 °C).

2.2.1. Garlic Additive Extraction Process

The extraction of (Garlic) involved using a concentration of 375 mg mL^{-1} chloroform and acetone solvent in the ratio of (80:20). The raw powder was mixed into 24 mL of chloroform and vortexed for 25 s, an addition of 10 mL acetone was added to separate the excess powder that was not dissolved into the chloroform. The solutions were then centrifuged for 15 min at a speed of 2000 rpm. Moreover, the solutions were allowed to settle for 24 h and the collected product was separated several times using a filter funnel.

2.2.2. Solution Rheology

The polymer solutions viscosity and surface tension were determined utilizing a calibrated Kruss tensiometer (Kruss GmbH, Hamburg, Germany) employing the standard Du Nouy ring method. Additionally, a Brookfield viscosity meter (AMETEK Brookfield, Harlow, UK) with an SCV-18 spindle attached was used. The tests were repeated three times at an ambient temperature of (≈23 °C).

2.3. Core-Sheath Fiber Mesh Generation

The core-sheath pressurized gyration apparatus used by Mahalingam et al.,[34,35] as depicted in (**Figure 1A**) was utilized to manufacture both core-sheath and singular-sheath fibers for the experiments conducted with PCL, PEO, PEO/Garlic, CS PEO/PCL and CS PEO/Garlic/PCL fibers. The equipment consists of a twin-reservoir pot with a 20 mL capacity and two concentric orifices on the wall of the vessel. The upper part of the vessel links to pressurized gas (N_2), while the lower part connects to a DC motor with a maximum speed of 6000 rpm. Polymer solutions were introduced into the vessel through the inlet and outlet opening on the lid of the vessel.

2.4. Design Features

The process of generating core-sheath fibers involved loading the inner vessel with a 3 mL volume of a 15% w/v virgin PCL polymer solution to serve as the core of the fibers. Simultaneously, the outer vessel was filled with a 3 mL volume of a 15% w/v PEO/Garlic polymer solution to serve as the fibers' sheath. For comparison, the PEO/Garlic polymer solution was added only to the core vessel, while the sheath remained empty, to obtain singular fibers for comparing drug release behavior. The polymer solutions were then spun for 60 s at a fixed pressure of 0.1 MPa in the vessel, generated by the flow of N_2 and a fixed rotating speed of 6000 rpm under ambient conditions (22 °C and ≈45–51% relative humidity) to form fibrous dressings depicted in (Figure 1B)(Participant involved in the study presented in Figure 1B provided their written informed consent). This process was repeated three times. The centrifugal force created by the high-speed rotational movement and flow pressure, ejects the polymer solutions through both inner and outer capillaries of the vessel, leading to the formation of a fiber patch as the solvent evaporates.[36]

2.5. Characterization

2.5.1. Fourier Transform Infrared Spectroscopy (FTIR)

The chemical properties of PEO, PCL, Garlic, PEO/Garlic, CS PEO/PCL and CS PEO/Garlic/PCL samples were analyzed using a Fourier Transform Infrared Spectrometer (FTIR, Nicolet iS50, Thermo Scientific, USA), equipped with an attenuated total reflectance (ATR) attachment, in the range of 4000–650 cm^{-1}. Data collection was performed over 32 scans at a resolution of 4 cm^{-1}. Obtained spectra were analyzed by overlapping to evaluate the functional differences between the sample groups.

2.5.2. Thermogravimetric Analysis (TGA)

Thermogravimetric (TGA) analysis (TA Instruments Q600-SDT, USA) was performed to investigate and compare the thermal stability and decomposition features of PEO, PCL, PEO/Garlic, CS PEO/PCL and CS PEO/Garlic/PCL samples. The analysis was carried out under nitrogen atmosphere fed at 100 mL min^{-1} purge. An increasing temperature ramp of 10 °C per minute was applied during the analysis, from ambient temperature to 600 °C.

2.5.3. Scanning Electron Microscopy (SEM)

The surface morphology of PCL, PEO, PEO/Garlic, CS PEO/PCL and CS PEO/Garlic/PCL fibers was analyzed using a scanning electron microscope (SEM, Hitachi S-3400n, Japan) with an accelerating voltage of 5 kV. The surface of the samples was coated with gold using a Quorum Technologies Q150R ES sputter coater for 90 s. Micrographs obtained from SEM imaging were analyzed using Image J software to determine the average fiber diameter and size distribution. For this study, 100 randomly selected fiber strands from each sample were measured for size. The average fiber diameter was calculated and plotted using Origin Pro software. A comparative analysis of all fiber samples was conducted using the diameter data.

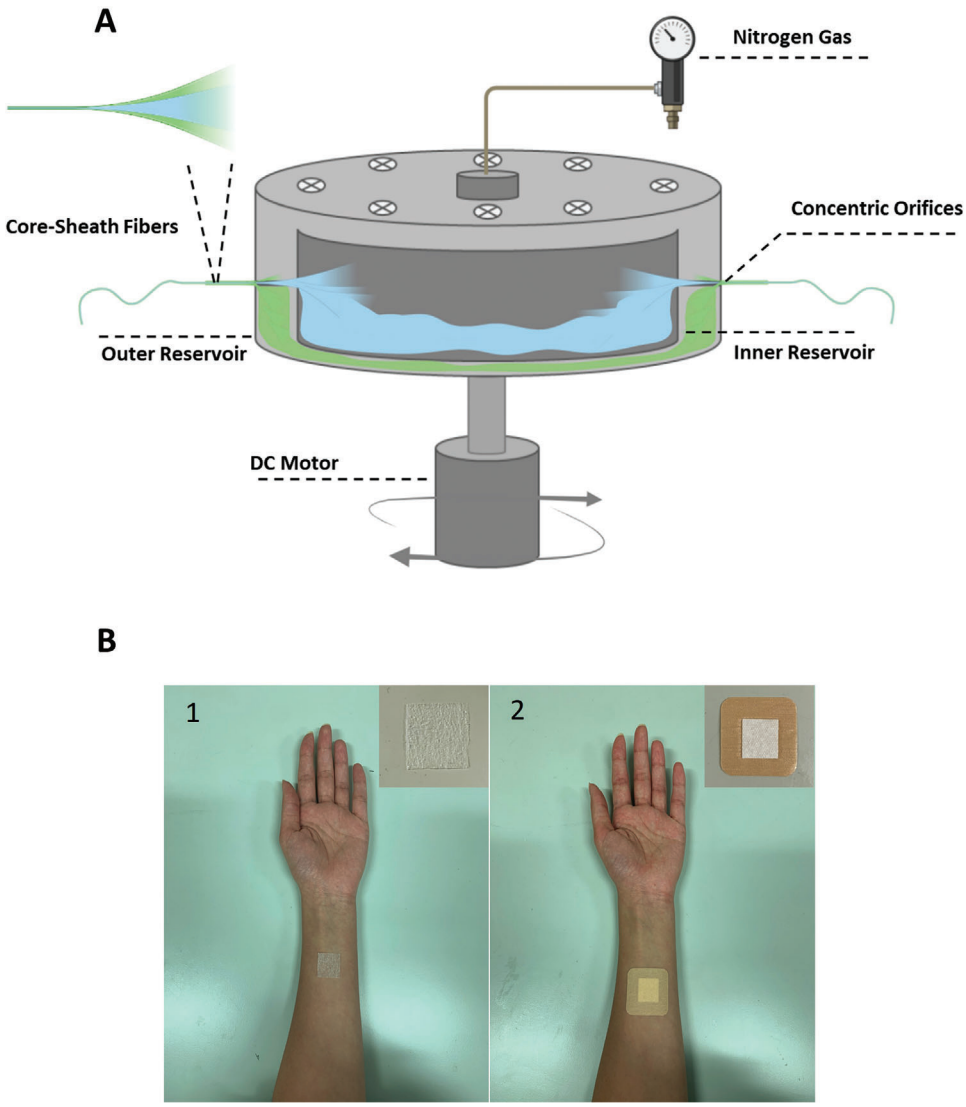

Figure 1. A) Schematic representation of core-sheath pressurized gyration set-up, B) 1-Photograph of the garlic extract fibrous wound dressing, 2-Garlic extract bandage fibrous with a waterproof protection layer, insets showing close-ups of the bandages' plaster (Participant involved in the study provided their written informed consent).

2.5.4. Loading of Garlic Additive and In-Vitro Release Study

PBS (pH = 7.4) was used as the test medium for in-vitro (Garlic) release assessment. The concentration of garlic in PBS was quantified using UV–Vis spectroscopy at a wavelength of 225 nm. Prior to the release study, a linear calibration curve was established based on a series of standard solutions with concentrations ranging from 5 to 100 mg mL^{-1}. The release study was conducted by placing 20mg of additive-loaded PEO/Garlic and PEO/Garlic/PCL fibrous patches into 20 mL PBS solution and incubated in a shaker at 37 °C. At predetermined time intervals, 2 mL of supernatant was removed from each assessment medium and replaced with 2 mL of fresh test medium to maintain the sink condition. The removed supernatants were filtered using 0.45 µm Millipore filter and assessed using a UV spectrophotometer. The data collected were used to calculate the cumulative release percentage of garlic additive. These experiments were carried out in triplicate ($n = 3$).

2.5.5. Cell Culture

PCL, PEO, PEO/Garlic, CS PEO/PCL and CS PEO/Garlic/PCL fibers were tested in accordance with the ISO10993-5 standard for "Biological evaluation of medical devices – Part 5: Tests for in-vitro cytotoxicity," with slight modifications. The fiber samples were tested using the ATCC dermal fibroblast cell line.[37] The samples were sterilized under UV light in sterile conditions. A constant sample-medium ratio of 6 cm^2 mL^{-1} was maintained according to the relevant standard. To each material, 6 mL of standard cell culture medium containing 90% DMEM (Dulbecco's Minimum Essential Medium), 10% FBS (Fetal Bovine Serum), 4

$\times 10^{-3}$ M L-glutamine and 100 IU mL^{-1} penicillin/streptomycin was added and incubated at 37 °C for 72 h. After 72 h, the culture medium of the dermal fibroblast cells, prepared in well plates 24 h prior, was replaced with the medium that had been incubated with fiber samples. Morphological changes in the cells were observed 24 h after the interaction. After 48 h, all samples were analyzed using the Annexin PI method on a Novocyte flow cytometer (Agilent Technologies, Santa Clara, CA, USA). RNA isolation was performed on all samples using an RNA isolation kit and quality controls were performed through spectrophotometric measurement.

2.5.6. Antibacterial Activity

Antibacterial activities of the CS PEO/PCL and CS PEO/Garlic/PCL fiber samples against the Gram-Positive *Staphylococcus aureus* (*S. aureus, ATCC #29213*) and Gram-Negative *Escherichia coli (E.coli, ATCC #25922)* bacteria species were tested using a bacterial adhesion/biofilm formation assay,[38] with samples prepared as 6 cm^2 patches ($n = 3$). Bacteria inoculum concentrations were adjusted to match the 0.5 McFarland turbidity standard and a bacteria concentration of $1{\times}10^8$ colony-forming units (CFU) was prepared. The fiber samples were immersed in well plate dishes and incubated for 24 h. Subsequently, the fiber samples were collected and sonicated in PBS for 15 min. The adhered bacteria were collected in the PBS solution and serially diluted. Eight serial dilutions were prepared and 100 µL droplets were applied to the agar using Mueller Hinton Agar medium. The petri dishes were incubated at 37 °C for 24 h. After the incubation period, bacteria colonies were counted for each sample. All test samples and each of the dilution factors of the fiber test samples were tested in triplicate ($n = 3$). Additionally, each of the fiber samples underwent a fixation procedure after 24 h of incubation with bacteria, using glutaraldehyde treatment for both *E. coli and S. aureus* bacteria species. Water was removed using ethanol–water mixture solutions (50, 60, 70, 80, 90, 95 and 100% v/v, respectively). The fiber samples were coated with gold sputter prior to analysis and examined by SEM.

2.5.7. Statistical Analysis

ANOVA: A single-factor test was used to determine the statistically significant differences among the diameters of PCL, PEO, PEO/Garlic, CS PEO/PCL and CS PEO/Garlic/PCL. Two-tailed *t*-tests were performed to evaluate the relative significance of drug release between PEO/Garlic and CS PEO/Garlic/PCL fibers and figures display the significance levels (*P*-values). Antibacterial activity of the fiber samples was statistically analyzed using a One-Way ANOVA and the Tukey test for multiple comparisons, with a significance level of ($p < 0.05$).

3. Results and Discussion

3.1. Fiber Morphology

The physical properties of polymer solutions are critical to the success of fiber production, as it can impact the morphology and the final properties of the fibers produced. The PEO/Garlic polymer solution has shown to have the highest surface tension compared to PCL and PEO (**Table 1**). In this case, the type of solvent used has a significant influence on the surface tension of the solution. PEO/Garlic's high surface tension can be attributed to the presence of garlic extract in the solution. Garlic extract is a polar compound and its addition to the PEO solution increases the overall polarity of the solution. This leads to stronger intermolecular forces between the molecules, thus, a higher surface tension. Additionally, the presence of acetone in the PEO/Garlic solution also contributes to the higher surface tension, as acetone is a more polar solvent than chloroform and can also increase the overall polarity of the solution. Nevertheless, the virgin PEO polymer solution still has a higher surface tension than PCL. This is due to hydrophilic polymers such as PEO having a high affinity for water which can increase the surface tension of a solvent when dissolved.

Table 1. Physical properties of PCL, PEO and PEO/Garlic polymer solutions.

Polymer	Concentration [%] w/v	Solvent	Surface Tension [mN m^{-1}]	Viscosity [mPa s]
PCL	15	Chloroform	29.9 ± 0.8	651.15 ± 64.3
PEO	15	Chloroform	46.8 ± 0.4	1649.67 ± 32.9
PEO/Garlic	15	Chloroform/Acetone	49.1 ± 0.9	4467.1 ± 31.8

On the other hand, the measured viscosities are influenced by the concentration of the polymer and the type of solvent used. PCL has the lowest viscosity among the tested polymers, while PEO/Garlic has the highest. This can be attributed to the higher molecular weight of PEO/Garlic, which results in stronger intermolecular forces and greater resistance to deformation. Furthermore, the addition of garlic extract to the PEO solution increases the molecular weight of the resulting PEO/Garlic polymer, which, in turn, increases the viscosity of the solution. This is due to garlic containing several hydrophilic components such as polysaccharides and proteins and having thickening properties. Additionally, the presence of acetone in the PEO/Garlic solution can also contribute to the higher viscosity, as acetone has a lower boiling point than chloroform and can evaporate more slowly, leading to a thicker, more viscous solution.

Figure 2 shows scanning electron micrographs of PCL, PEO, PEO/Garlic, CS PCL/PEO and CS PEO/Garlic/PCL fibers generated at a working pressure of 0.1 MPa and a rotational speed of 6000 rpm. PCL fibers showed an average diameter of 2.9 µm ± 1.1 µm. The gyrospun fibers obtained were mostly aligned, with nanopores on the surface, resulting from the use of a volatile solvent such as chloroform (Figure 2A). The PEO fibers had an average diameter of 0.8 µm ± 0.3 µm with a smooth surface structure (Figure 2B). Similarly, the PEO/Garlic fibers, generated at a production rate of 162 g h^{-1}, had an average diameter of 0.8 µm ± 0.2 µm (Figure 2C); however, the fibers were curly, unaligned and exhibited a bead-on-string morphology. The bead-on-string morphology is thought to be caused by uneven solvent evaporation along the fiber chain. Beaded structures are known to be beneficial in drug delivery applications where the beads can be utilized to incorporate additives, in this case (Garlic extract). The

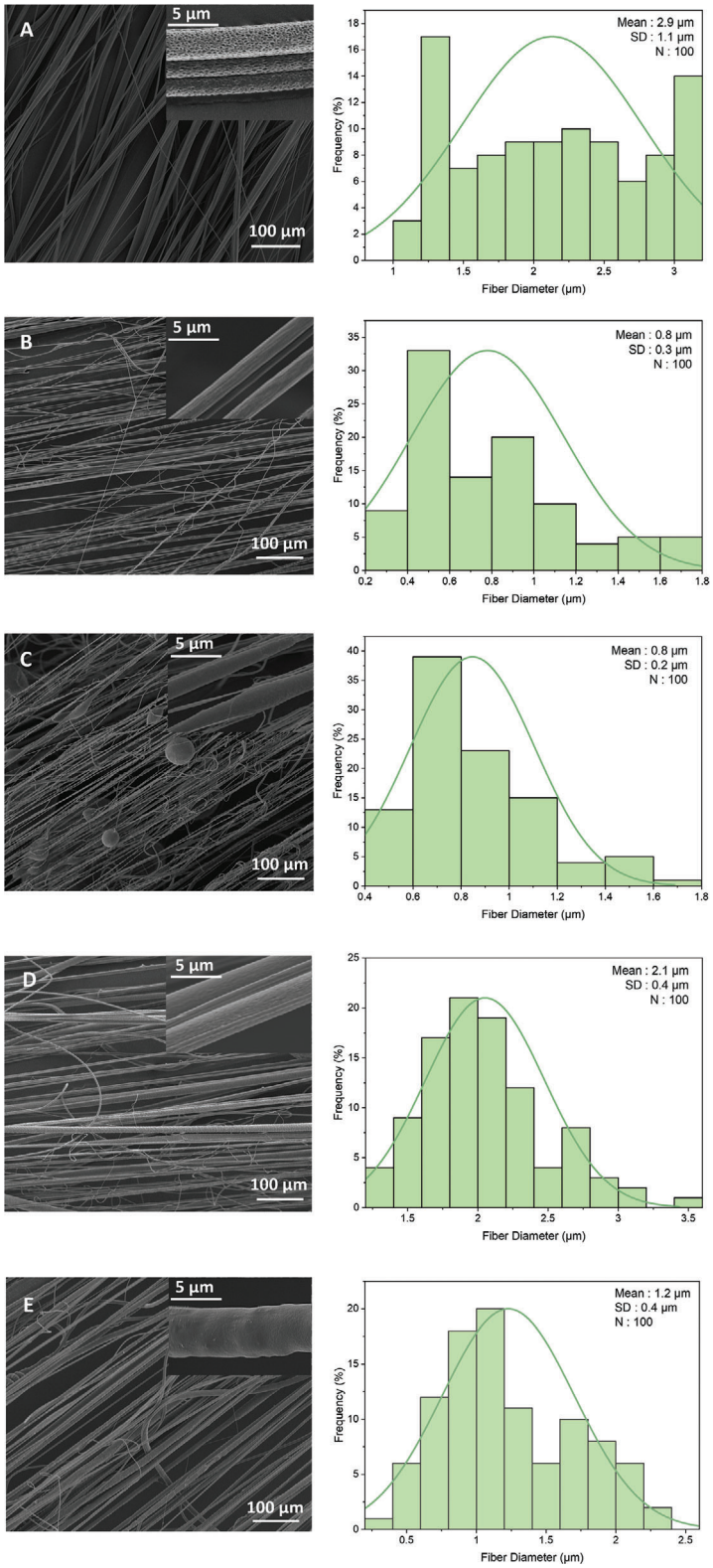

Figure 2. SEM images and size distribution graphs of: A) PCL, B) PEO, C) PEO/Garlic, D) CS PEO/PCL, and E) CS PEO/Garlic/PCL fiber samples. Statistically significant difference between all fiber groups ($p < 0.05$). Inset micrographs on the right-hand side of each image show the high magnification scenario.

Table 2. Production rate of PEO/Garlic and CS PEO/Garlic/PCL meshes.

Polymer	Concentration [%] w/v	Solvent	Production Rate [g h^{-1}]
PEO/Garlic	15	Chloroform/Acetone	162
PEO/Garlic/PCL	15	Chloroform/Acetone	180

CS PEO/PCL fibers exhibited an increased diameter compared to the PEO/Garlic fibers, 2.1 µm ± 0.4 µm (Figure 2D), which was similar to the diameter of PCL fibers. The topography of these fibers also exhibited a smooth surface, which is the result of having PEO in the sheath and PCL in the core structure. Surprisingly, the addition of garlic in the CS PEO/Garlic/PCL fibers, generated at a production rate of 180 g h^{-1} (**Table 2**), exhibited a different morphology in comparison to PEO/Garlic, as the fibers were bead-free, which could be due to the addition of PCL in the core with a diameter of 1.2 µm ± 0.4 µm (Figure 2E). Overall, it can be concluded that the encapsulation of the garlic additive has decreased the fiber diameter. A decrease in fiber diameter results in a greater surface area to volume ratio, which promotes fibroblast, epithelial cell attachment and proliferation.

3.2. Thermal Stability

Thermogravimetric analysis (TGA) was used to analyze the thermal decomposition temperature and weight loss of PCL, PEO, PEO/Garlic, CS PEO/Garlic/PCL and CS PEO/PCL fibers. In all fiber samples, a multitype mass loss pattern was observed. TGA results showed that all the polymeric fiber samples had a one-step degradation profile (**Figure 3**). Degradation began at 379 °C for virgin PCL fibers through ester pyrolysis and unzipping depolymerization reactions, resulting in the rupture of their chains. The degradation of PEO fibers occurred very rapidly in one single step until 420 °C with thermal decomposition starting at 376 °C, leaving virtually no residue. Furthermore, the decomposition temperature of PEO/Garlic started at 378 °C and ended at 414 °C, which is slightly higher than that of PEO fibers. Additionally, the presence of garlic extract increased the thermal stability of PEO. However, a different situation is observed for the CS PEO/Garlic/PCL fibers, as the decomposition profile starts earlier at 358 °C and finishes at 416 °C, which shows that the presence of both polymers and the encapsulated garlic extract has decreased the thermal stability. Moreover, PCL core degrades at a lower temperature in the CS PEO/Garlic/PCL structure compared to virgin PCL fibers. A potential reason behind this is the mechanical pressure and heat transmission from the sheath PEO/Garlic to the core PCL, causing the core to degrade rapidly. Another cause is the high surface-volume ratio of the core and sheath, which enhances heat transmission even further. Furthermore, CS PEO/PCL fibers exhibited thermal decomposition starting at 378 °C and ending at 418 °C, which was the average of PEO and PCL fibers' decomposition individually.

3.3. Fiber Chemistry

To further characterize the fibers and confirm garlic additive entrapment FTIR analyses were conducted. The spectra of the garlic powder, PEO, PCL, PEO/Garlic, CS PEO/PCL and CS PEO/Garlic/PCL fibers were characterized by transmittance bands (**Figure 4**). The FTIR spectrum of garlic powder showed a broad peak at 3425 cm^{-1}. The peak corresponds to the stretching vibration of O–H from the hydroxyl group, confirming the existence of polyhydroxy substances such as flavonoids, non-flavonoids and saponins. These compounds contribute to garlic's antioxidant properties. The frequency at 2937 cm^{-1} belongs to the

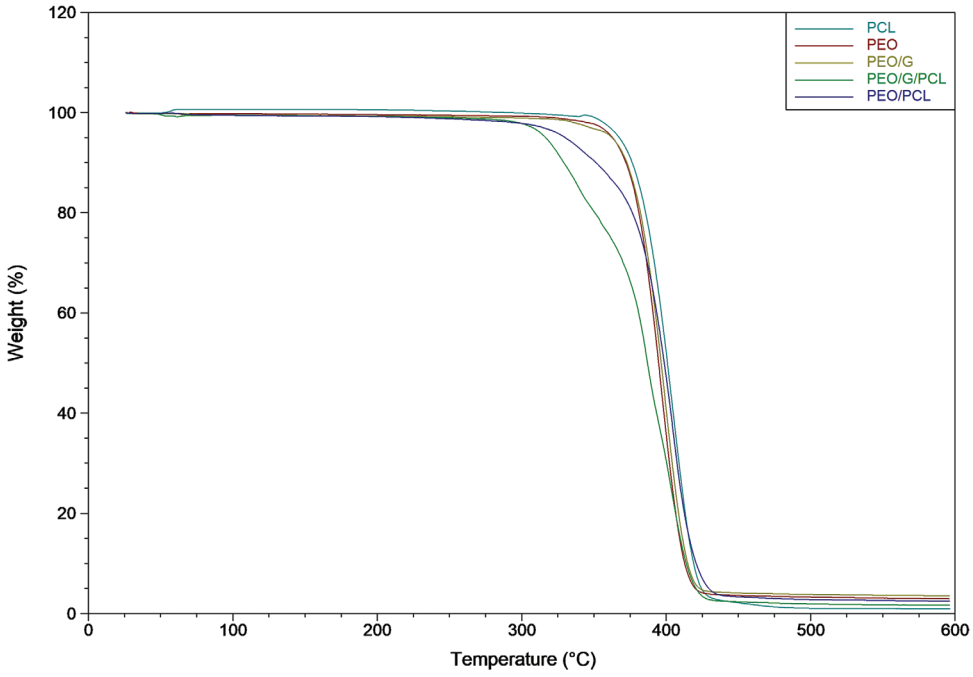

Figure 3. Thermograms of PCL, PEO, PEO/Garlic, CS PEO/Garlic/PCL, and CS PEO/PCL fiber samples.

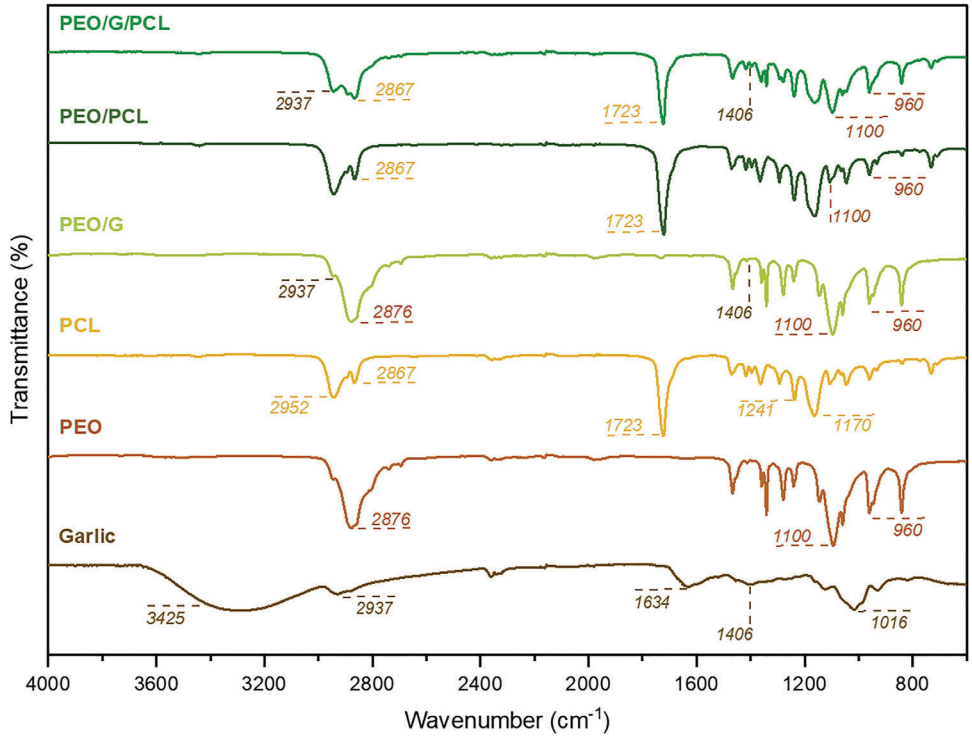

Figure 4. FTIR Spectra of Garlic powder, PCL, PEO, PEO/Garlic, CS PEO/Garlic/PCL, and CS PEO/PCL fiber samples.

asymmetric stretching of C–H in aromatic compounds (mainly lipids). The stretching of C═O from the carbonyl and carboxylate groups is shown by the peak at 1634 cm^{-1}, but the bending vibrations of O–H in carboxylic acids indicate the existence of flavonoids, tannins, saponins and glycosides which are represented by the peak at 1406 cm^{-1}. Moreover, tannins, saponins and glycosides are recognized as the antibacterial constituent in garlic powder. The strong signal at 1016 cm^{-1} is typical of garlic, indicating the S═O group and demonstrating the presence of organosulfur compounds such as alliin, allicin and diallyl disulfide.[17,39–42] PEO fibers showed characteristic peaks at 2876 cm^{-1} which is caused by molecular stretching of the methylene group CH_2, whereas the peaks at 1100 and 958 cm^{-1} are caused by stretching of the ether group in PEO which is further indicated as the C–O–C absorption complex. The complex is made up of three distinct, though sometimes overlapping, summits. The C–O–C complex is particularly sensitive to varied chain conformations that may be found in semicrystalline polymers such as PEO.[43–45] Moreover, PCL fibers confirmed the typical bands of CH_2 asymmetric stretching at 2952 cm^{-1} and symmetric stretching at 2867 cm^{-1}. The sharp C═O characteristic bands at 1723 cm^{-1} was obtained due to ester carbonyl group. Additionally, the peaks at 1241 cm^{-1} are associated with C–O–C stretching, whereas band 1170 cm^{-1} is related with C–O stretching.[46–48] The distinctive absorption peak in the CS PEO/PCL and CS PEO/Garlic/PCL fiber matrix spectrum corresponded with that observed in the PEO and PCL spectra, implying that PEO and PCL were not bound during core-sheath spinning, indicating that the core and sheath layers were physically connected into fibers. Nevertheless, no new characteristic peaks were found in the fibers' spectra following garlic additive loading. Two factors could have led to this finding, one can be that some bands overlapped between the characteristic bands of garlic additive and those of the polymers; another can be that the additive concentration in the fibers was low. Furthermore, this demonstrated that the garlic additive and polymer matrix were only physically combined and therefore retained their characteristics. Nevertheless, the presence of the garlic additive in the CS PEO/Garlic/PCL and PEO/Garlic spectra can still be indicated as the bands slightly differ from CS PEO/PCL and PEO fibers spectra.

3.4. In-Vitro Release

The evaluation of novel core-sheath fibers containing a PCL core and a PEO/G sheath is studied, for the localized delivery of natural antibacterial agents for the treatment of minor cuts and wounds. The incorporation of garlic within the hydrophilic PEO sheath was intended to utilize its well-established antibacterial properties to reduce the risk of infection during the early phases of wound care, where infection risks are at their highest. While the hydrophobic PCL core was chosen for its biocompatibility and structural integrity, thus providing a stable scaffold that supports cell attachment and proliferation. The in-vitro release profiles of the fibers were assessed in PBS at (pH = 7.4) mimicking physiological conditions at a body temperature of (37 °C). Comparative analysis indicated a slightly different release profile between both fibers, PEO/G versus CS PEO/G/PCL, over a 240-min assessment period. Several factors such as fiber structural integrity, properties of the developed materials, garlic loading concentration as well as solubility profiles of the polymers involved, were identified as critical factors affecting the garlic extract diffusion.

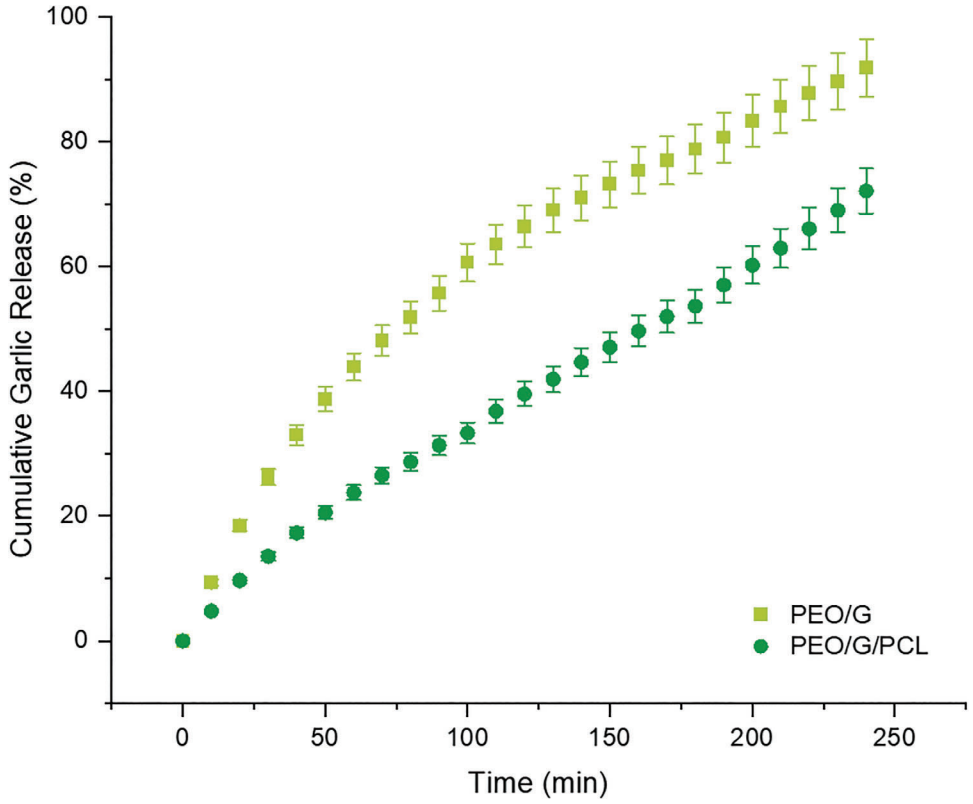

Figure 5. Garlic extract released from fiber patches of PEO/Garlic and CS PEO/Garlic/PCL samples ($p < 0.05$).

Although, the garlic additive was incorporated in PEO for both singular PEO/G and CS PEO/G/PCL fibers, the initial release profile proved to be different. PEO/G fiber patches showed an initial release of 43% in the first 60 min, whereas CS PEO/G/PCL fibers showed an initial release of 23%. PEO/G fibers rate of release rapidly reached 66% in 120 min while CS PEO/G/PCL followed by a slower release rate of 39%. Both samples demonstrated a rapid release pattern at varying rates. PEO fibers have a specific hydration response upon contact with water, absorbing it rapidly and swelling. This swelling can cause the fiber diameter to expand, leading to changes in mechanical properties. Moreover, the swelling may influence the diffusion of the garlic additive out of the fiber matrix, potentially affecting both the rate and quantity of additive release. Furthermore, PEO/G exhibited a faster release profile, with a maximum release of 91%, in comparison to CS PEO/G/PCL, which only achieved a 72% release within 240 min (**Figure 5**).

Statistical analyses confirmed a significant difference ($p < 0.05$) in the release profiles between the PEO/G and CS PEO/G/PCL fibers. The rapid yet sustained release of garlic from both samples was an expected behavior of the singular and core-sheath structures, as the garlic additive was loaded into the sheath layer on the surface of the fibers and the carrier of the extract is a water-soluble polymer. The current findings illustrate the potential of core-sheath fibers to serve as novel wound dressings (plasters), offering immediate potent antibacterial action that prevents infection, followed by a long-lasting, cell-friendly scaffold that can accelerate the healing of minor cuts and wounds.

It is well stablished in literature that the release of active ingredients from PEO matrices is controlled by the PEO taking up water to form a gel and the release of the active ingredient from the gel, potentially involving dissolution of the gel. Measurements in the present study suggest that the amount of PEO dissolved during the release experiments was 10%, so it is appropriate to assume release from a gel without dissolution and to fit the data with a first-order profile, in which the fractional release $\varphi(t)$ as a function of time t is

$$\varphi(t) = 1 - \exp(-at) \tag{1}$$

where a is a constant which combines the effect of transport through the gel, transfer from the gel to the release medium and transport from the surface of the particles to the bulk of the fluid. The results of fitting are shown in (**Figure 6**): the quality of the fits may be described by the corrected Akaike information criterion (AICc) or R^2. For the PEO/Garlic fibers we find $a = 0.0092$ min^{-1} with [AICc,R^2] = [94.20, 0.99676] and for CS PEO/Garlic/PCL fibers $a = 0.0045$ min^{-1} with [AICc, R^2] = [115.1, 0.98818]. A better fit to the core-sheath fibers can be obtained with a function of the form.

$$\varphi(t) = r(1 - \exp(-at)) \tag{2}$$

giving [AICc, R^2] = [98.20, 0.99459] with $a = 0.0026$ min^{-1}, but as the fit results in $r = 1.48 > 1$, which is unphysical, we reject this. On examining the residuals from the fit, we perceive that the fit slightly underestimates the release for about the

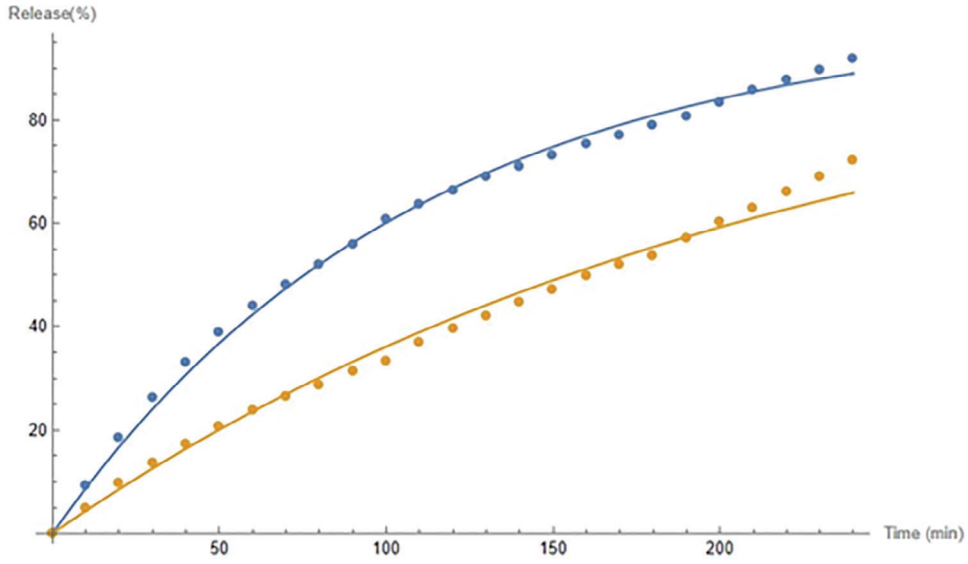

Figure 6. Fit of a first-order release model for PEO/Garlic fibers (blue) and for CS PEO/Garlic/PCL fibers (orange).

first hour, overestimates it for the next two hours and slightly underestimates it thereafter. The model in its present form agrees well with the experimental results.

3.5. Cell Culture

Dermal fibroblast cell lines were used to test samples of PCL, PEO, PEO/G, CS PEO/PCL and CS PEO/G/PCL fibers to determine whether they caused any negative side effects or toxicity to the surrounding tissue when used as a natural plaster in integrative medicine applications. The number of dead, live and apoptotic cells were counted and used to calculate percentage ratios. The ratio of live cells to the total number of cells determined the cell viability ratio and the cellular response to the fiber samples. The results of the cell studies are presented in (**Figure** 7A–B). The results showed that no toxic effect was observed in any of the fiber samples in the presence of garlic. The cell viability percentage for the control group was determined to be 92.40%. However, PEO Virgin fiber samples exhibited a cell viability of 58.65%, which

A

	Control		PEO Virgin		PCL Virgin		CS PEO/PCL		PEO/G		CS PEO/G/PCL	
	Count	%	Count	%	Count	%	Count	%	Count	%	Count	%
TOTAL CELL	34,194	30.20%	7,230	15.04%	25,289	23.27%	23,520	30.74%	34,256	4.05%	31,764	22.58%
DEAD CELL	1,622	4.78%	1,717	27.81%	1,341	5.46%	747	3.21%	961	2.86%	1,971	6.32%
LIVE CELL	31,331	**92.40%**	3,621	**58.65%**	22,461	**91.38%**	22,049	**94.80%**	31,847	**94.76%**	28,442	**91.15%**
APOPTOTIC CELL	856	2.52%	417	6.75%	603	2.45%	329	1.41%	613	1.82%	743	2.38%

B

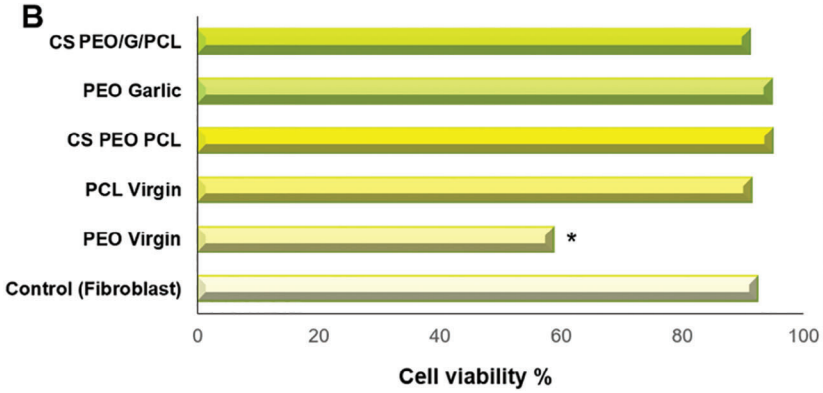

C

Sample	RNA Concentration(ng/ul)
Control (Fibroblast)	263,8
PEO Virgin	253,8
PCL Virgin	98,0
CS PEO PCL	200,1
PEO/Garlic	214,1
CS PEO/G/PCL	215,3

Figure 7. Cell viability analysis of PCL, PEO, PEO/Garlic, CS PEO/PCL, and CS PEO/Garlic/PCL samples (*, $p < 0.05$).

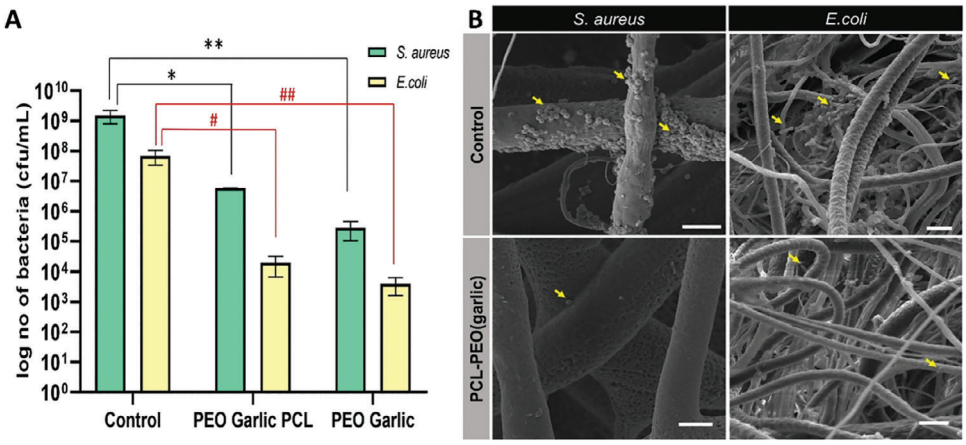

Figure 8. Antibacterial analysis of A) Bacterial adherence (*S. aureus* and *E. coli*) test results of control, CS PEO/PCL and CS PEO/Garlic/PCL (*, **, # and ## exhibit the statistically significance, $p < 0.05$). SEM images of *S. aureus* and *E. coli* bacteria species adhered on to B) CS PEO/PCL and CS PEO/Garlic/PCL fiber samples (scale bars = 5 μm).

was lower than that of the other fiber samples. Although PEO is a biocompatible polymer, it dissolves completely in the cell culture medium owing to its hydrophilicity, thus losing its integrity. Additionally, the quantity of the sample negatively impacts the cells' metabolic activity, decreasing the viability percentage. Jamil and co-workers [49] reported that PEO nanofibers with 5%, 6% and 7% PEO concentrations showed varying cell culture results, with increased PEO concentration (7% PEO) reducing the cell viability of MCF-7 breast cancer cell lines by up to 50%. The addition of garlic to PEO fibers increased cell viability up to 94.76% in PEO/G fiber samples. The presence of garlic eliminated the negative effect on cell metabolism caused by high PEO concentrations. Furthermore, the solubility-lowering effect of garlic on PEO positively influenced the preservation of cell viability. Also, RNA was isolated from all samples and evaluated by correlating it with the total number of cells (Figure 7C). RNA concentration was calculated to be 263.8 ng uL^{-1}, correlating with the highest total cell number in the control group.

PCL Virgin and CS PEO/PCL fiber samples showed cell viability percentages of 91.38% and 94.80%, respectively. PCL is a hydrophobic, biocompatible and biodegradable polymer.[50] When PEO was combined with PCL in a core-sheath structure, the total concentration of PEO in cell culture media decreased and no toxic effects were observed. Additionally, considering all these factors, CS PEO/G/PCL fibers demonstrated high cell viability without any toxic effects. The resultant core-sheath structure, incorporating garlic, exhibited a cell viability of 91.15%. The ratios of apoptotic cells were lower than those of dead cells, being 7%, indicating that the cells were healthy. As a result, it was concluded that the garlic-containing hydrophilic/hydrophobic core-sheath fiber samples have cell-compatible characteristics for integrative medicine applications, without causing any side effects on the surrounding tissue.

3.6. Antibacterial Activity

Antibacterial activity of the core-sheath samples was tested using the bacterial adhesion test for biofilm formation. Cell viability test results indicated that an increasing amount of PEO content showed cytotoxicity above a threshold amount of dissolved PEO. Additionally, a lower PEO amount with garlic additive showed increased cell viability. Considering these results and according to the main aim of the study, CS PEO/PCL and CS PEO/Garlic/PCL samples were comparatively tested for their antibacterial activity using *S. aureus* and *E. coli* bacteria species. The results showed that both CS PEO/PCL and CS PEO/Garlic/PCL samples exhibited antibacterial activity up to 4 orders of magnitude compared to the control group for both gram-positive and gram-negative bacteria species (**Figure** 8A). Biofilm test results demonstrated a statistically significant decrease in the number of adhered bacteria for both CS PEO/PCL and CS PEO/Garlic/PCL samples compared to the control group for each of the bacteria species. In the control group of *S. aureus*, a 1.5×10^9 log bacterial count (cfu mL^{-1}) was measured, whereas 6×10^6 and 2.9×10^5 log numbers (cfu mL^{-1}) of adherent bacteria were determined for CS PEO/PCL and CS PEO/Garlic/PCL samples, respectively. According to the antibacterial test results, CS PEO/PCL fibers reduced biofilm formation by approximately log 3 compared to the control group, while the antibacterial activity increased to log 4 with the addition of garlic to the upper layer of CS fibers (CS PEO/Garlic/PCL). The control group of *E. coli* was measured as $\approx7\times10^7$ log bacterial count (cfu mL^{-1}). Moreover, $\approx1.7\times10^4$ and 4×10^3 log numbers (cfu mL^{-1}) of adhered *E. coli* were determined for CS PEO/PCL and CS PEO/Garlic/PCL samples, respectively. The same decrease ratio with *S. aureus* tests log 3 for CS PEO/PCL and log 4 for CS PEO/Garlic/PCL fibers were determined, respectively.

CS PEO/Garlic/PCL exhibited a log 1 decrease in bacterial adhesion compared to the CS PEO/PCL fibers for both *S. aureus* and *E. coli*. SEM micrographs of CS PEO/PCL and CS PEO/Garlic/PCL fiber samples supported the antibacterial test results. Representative images are presented in (Figure 8B) (scale bar = 5 μm). CS PEO/PCL fiber samples hosted higher amounts of bacterial adhesion compared to CS PEO/Garlic/PCL. Antibacterial activity of core-sheath samples was achieved through dual strategies: the first is the degradation potential of PEO, which aids in inhibiting bacterial adherence and the second, the main

strategy, involves the release of garlic extract, a well-established antibacterial compound due to its organosulfur compound content. The obtained results support the antibacterial properties of garlic.[51] Antibacterial biomaterials developed using natural extracts such as garlic offer cost-effective and safe alternative solutions, especially against bacteria that have developed antibiotic resistance, given their biocompatible nature and high activity.

4. Conclusions

The use of garlic as a source of natural compounds with superior therapeutic properties has been explored. A core-sheath fiber composite structure was designed and mass-produced using PCL in the core layer and PEO (Garlic) as the sheath layer, this has been found to provide high mechanical strength, long-term stability, high antibacterial activity and cell-friendly surface properties. The addition of garlic extract to PEO fibers was shown to decrease fiber diameter and enhance the thermal stability of the fibers. The biocompatibility of the fiber samples was evaluated; the results showed that they are safe and nontoxic to surrounding tissues. Furthermore, they have no negative effects on cell viability or metabolism, making them suitable for integrative medicine applications. In-vitro tests proved that the fibers can be used for local natural additive delivery. The PEO/Garlic fibers exhibited a faster initial release pattern compared to CS PEO/Garlic/PCL fibers, suggesting that the latter may have a longer-lasting effect. The core-sheath structure ensures that upon application as a plaster, there is an initial burst release of garlic from the PEO sheath to stop the microorganism growth. Followed by the gradual dissolution of the PEO, the underlying PCL core is exposed, providing a supportive matrix that encourages micromovement, a crucial factor in promoting cellular attachment and tissue regeneration. Further analysis of the study indicated that the physical properties of the polymer solutions play a crucial role in the fiber production process and affect the morphology and properties of the final product. In conclusion, the high cell viability observed in the in-vitro study suggests that these core-sheath fibers have the potential to promote wound healing in a safe and effective manner. This approach broadens the possible uses of multicomponent natural agent polymeric systems, bypassing the need to find a single material that fits all the required parameters. Besides, the mass production of these fibers at a rate of 162–180 g h^{-1} using the core-sheath pressurized gyration demonstrates the feasibility of cost-effective manufacturing. Therefore, incorporation of a natural therapeutic agent in a multicomponent system such as core-sheath structures produced via core-sheath pressurized gyration is a promising approach for the development of cost-effective, sustainable, highly effective antibacterial and nontoxic wound dressings.

Acknowledgements

The UCL authors are grateful to EPSRC for funding pressurized gyration research (grants: EP/S016872/1, EP/N034228/1, EP/L023059/1). The authors would also like to express their deep gratitude to Hacettepe University Advanced Technologies Application and Research Centre for the infrastructure facilities provided during the characterization part of the study. H.M. thanks the Persia Educational Foundation (Mirzakhani Scholarship) for supporting her Ph.D. studies at University College London.

Conflict of Interest

The authors declare no conflict of interest.

Data Availability Statement

The data that support the findings of this study are available from the corresponding author upon reasonable request.

Keywords

antibacterial, cell-compatible, garlic plasters, naturopathic healthcare, wound healing

Received: January 14, 2024
Revised: March 24, 2024
Published online:

[1] M. S. Criollo-Mendoza, L. A. Contreras-Angulo, N. Leyva-López, E. P. Gutiérrez-Grijalva, L. A. Jiménez-Ortega, J. B Heredia, *Molecules* **2023**, *28*, 598.
[2] S. Huang, X. Fu, *J. Controlled Release* **2010**, *142*, 149.
[3] W. Czaja, A. Krystynowicz, S. Bielecki, R. Brownjr, *Biomaterials* **2006**, *27*, 145.
[4] V. Andreu, G. Mendoza, M. Arruebo, S. Irusta, *Materials* **2015**, *8*, 5154.
[5] C. Liao, Y. Li, S. C. Tjong, *Int. J. Mol. Sci.* **2019**, *20*, 449.
[6] A. P. Ingle, N. Duran, M. Rai, *Appl. Microbiol. Biotechnol.* **2014**, *98*, 1001.
[7] R. F. Pereira, P. J. Bartolo, *Adv. Wound Care* **2016**, *5*, 208.
[8] S. Durairaj, S. Srinivasan, P. Lakshmanaperumalsamy, *Electron. J. Biol.* **2009**, *5*, 5.
[9] Y. S. de Queiroz, P. B. Antunes, S. J. V. Vicente, G. R. Sampaio, J. Shibao, D. H. M. Bastos, E. A. F. S. Torres, *Int. J. Food Sci. Technol.* **2014**, *49*, 1308.
[10] B. R. Gudalwar, M. G. Nimbalwar, W. A. Panchale, A. B. Wadekar, J. V. Manwar, R. L. Bakal, *GSC Adv. Res. Rev.* **2021**, *6*, 220.
[11] M. H. Pittler, E. Ernst, *Mol. Nutr. Food Res.* **2007**, *51*, 1382.
[12] A. Tesfaye, W. Mengesha, *Int. J. Sci. Res. Eng. Technol.* **2015**, *1*, 142.
[13] M. Sharma, A. Gupta, R. Prasad, *Int. J. Res. Rev.* **2017**, *4*, 103.
[14] S. Saifzadeh, A. Tehrani, F. S. S. Jalali, R. Oroujzadeh, *J. Anim. Vet. Adv.* **2006**, *5*, 1101.
[15] A. A. El-Refai, G. A. Ghoniem, A. Y. El-Khateeb, M. M. Hassaan, *J. Nanostruct. Chem.* **2018**, *8*, 71.
[16] W. A. Sarhan, H. M. Azzazy, I. M. El-Sherbiny, *ACS Appl. Mater. Interfaces* **2016**, *8*, 6379.
[17] D. Edikresnha, T. Suciati, M. M. Munir, K. Khairurrijal, *RSC Adv.* **2019**, *9*, 26351.
[18] S. G. Er, T. A. Tabish, M. Edirisinghe, R. K. Matharu, *Front. Med.* **2022**, *9*, 3466.
[19] Y. Qing, L. Cheng, R. Li, G. Liu, Y. Zhang, X. Tang, J. Wang, H. Liu, Y. Qin, *Int. J. Nanomed.* **2018**, *13*, 3311.
[20] A. K. Chatterjee, R. Chakraborty, T. Basu, *Nanotechnology* **2014**, *25*, 135101.
[21] Y. Cui, Y. Zhao, Y. Tian, W. Zhang, X. Lü, X. Jiang, *Biomaterials* **2012**, *33*, 2327.
[22] E. Abiy, A. Berhe, *J. Infect. Dis.* **2016**, *2*, 1.
[23] M. R. Farahpour, S. Hesaraki, D. Faraji, R. Zeinalpour, M. Aghaei, *J. Pharm. Sci.* **2017**, *53*, e15079.
[24] S. Mahalingam, R. Matharu, S. Homer-Vanniasinkam, M. Edirisinghe, *Appl. Phys. Rev.* **2020**, *7*, 041302.

[25] H. Majd, A. Harker, M. Edirisinghe, M. Parhizkar, *J. Drug Deliv. Sci. Technol.* **2022**, *72*, 103359.
[26] E. Altun, J. Ahmed, M. Onur Aydogdu, A. Harker, M. Edirisinghe, *Eur. Polym. J.* **2022**, *173*, 111300.
[27] A. Kurella, N. B. Dahotre, *J. Biomater. Appl.* **2005**, *20*, 5.
[28] G. Ciardelli, V. Chiono, G. Vozzi, M. Pracella, A. Ahluwalia, N. Barbani, C. Cristallini, P. Giusti, *Biomacromolecules* **2005**, *6*, 1961.
[29] L. Ghasemi-Mobarakeh, M. P. Prabhakaran, M. Morshed, M.-H. Nasr-Esfahani, S. Ramakrishna, *Biomaterials* **2008**, *29*, 4532.
[30] M. Rubert, J. Dehli, Y.-F. Li, M. B. Taskin, R. Xu, F. Besenbacher, M. Chen, *J. Mater. Chem. B* **2014**, *2*, 8538.
[31] A. Afshar, M. Gultekinoglu, M. Edirisinghe, *Int. Mater. Rev.* **2022**, *68*, 1.
[32] L. Li, H. Li, Y. Qian, X. Li, G. K. Singh, L. Zhong, W. Liu, Y. Lv, K. Cai, L. Yang, *Int. J. Biol. Macromol.* **2011**, *49*, 223.
[33] A. Afshar, H. Majd, A. Harker, M. Edirisinghe, *J. Drug Deliv. Sci. Technol.* **2024**, *95*, 105582.
[34] S. Mahalingam, S. Homer-Vanniasinkam, M. Edirisinghe, *Mater. Des.* **2019**, *178*, 107846.
[35] S. Mahalingam, S. Huo, S. Homer-Vanniasinkam, M. Edirisinghe, *Polymers* **2020**, *12*, 1709.
[36] Y. Dai, J. Ahmed, M. Edirisinghe, *Macromol. Mater. Eng.* **2023**, *308*, 2300033.
[37] M. Gultekinoglu, Y. Tunc Sarisozen, C. Erdogdu, M. Sagiroglu, E. A. Aksoy, Y. J. Oh, P. Hinterdorfer, K. Ulubayram, *Acta Biomater.* **2015**, *21*, 44.
[38] M. Gultekinoglu, B. Kurum, S. Karahan, D. Kart, M. Sagiroglu, N. Ertas, A. Haluk Ozen, K. Ulubayram, *Mater. Sci. Eng., C* **2017**, *71*, 1166.
[39] J. P. Reddy, J.-W. Rhim, *J. Nat. Fibers* **2018**, *15*, 465.
[40] A. Ardi, A. Fauzi, A. Rajak, K. Khairurrijal, *Mater. Today Proc.* **2021**, *44*, 3403.
[41] A. M. Youssef, H. S. El-Sayed, I. EL-Nagar, S. M. El-Sayed, *RSC Adv.* **2021**, *11*, 22571.
[42] D. Nagarajan, T. R. Kumar, *Int. J. Zool. Stud.* **2017**, *2*, 11.
[43] I. Pucić, T. Jurkin, *Radiat. Phys. Chem.* **2012**, *81*, 1426.
[44] P. L. Rockwell, M. A. Kiechel, J. S. Atchison, L. J. Toth, C. L. Schauer, *Carbohydr. Polym.* **2014**, *107*, 110.
[45] S. Wongsasulak, K. M. Kit, D. J. McClements, T. Yoovidhya, J. Weiss, *Polymer* **2007**, *48*, 448.
[46] T. Elzein, M. Nasser-Eddine, C. Delaite, S. Bistac, P. Dumas, *J. Colloid Interface Sci.* **2004**, *273*, 381.
[47] A. Garton, M. Aubin, R. E. Prud'Homme, *J. Polym. Sci. Polym. Lett. Ed.* **1983**, *21*, 45.
[48] N. Nagiah, R. Johnson, R. Anderson, W. Elliott, W. Tan, *Langmuir* **2015**, *31*, 12993.
[49] M. Jamil, I. S. Mustafa, N. M. Ahmed, S. B. Sahul Hamid, *Biomater. Adv.* **2022**, *143*, 213178.
[50] M. A. Elnaggar, H. A. El-Fawal, N. K. Allam, *Mater. Sci. Eng., C* **2021**, *119*, 111550.
[51] S. B. Bhatwalkar, R. Mondal, S. B. N. Krishna, J. K. Adam, P. Govender, R. Anupam, *Front. Microbiol.* **2021**, *12*, 1869.